

AD-769 860

INVESTIGATION OF LASER PROPAGATION
PHENOMENA

S. A. Collins, Jr.

Ohio State University

Prepared for:

Rome Air Development Center

September 1973

DISTRIBUTED BY:

NTIS

National Technical Information Service
U. S. DEPARTMENT OF COMMERCE
5285 Port Royal Road, Springfield Va. 22151

**Best
Available
Copy**

ADDC TR-15-20
Technical Report
September 1957

INVESTIGATION OF LASER PREPARATION TECHNIQUE

AD 769860

The Ohio State University
ElectroScience Laboratory

Department of Electrical Engineering
Columbus, Ohio 43210

Sponsored by
Defense Advanced Research Projects Agency
AFDA Order No. 127

Approved for public release
distribution unlimited.



The views and conclusions contained in this document are those of the authors and should not be interpreted as necessarily representing the official policies, either expressed or implied, of the Defense Advanced Research Projects Agency or the U. S. Government.

Reproduced by
NATIONAL TECHNICAL
INFORMATION SERVICE
U S Department of Commerce
Springfield VA 22151

Naval Air Development Center
Air Force Systems Command
Office of Procurement, New York

UNCLASSIFIED

SECURITY CLASSIFICATION OF THIS PAGE (When Data Entered)

REPORT DOCUMENTATION PAGE		READ INSTRUCTIONS BEFORE COMPLETING FORM
1. REPORT NUMBER RADC-TR-73-321	2. GOVT ACCESSION NO.	3. RECIPIENT'S CATALOG NUMBER
4. TITLE (and Subtitle) Investigation of Laser Propagation Phenomena		5. TYPE OF REPORT & PERIOD COVERED Quarterly 1 Apr 73 - 30 Jun 73
		6. PERFORMING ORG. REPORT NUMBER Electroscience Lab 5432-6
7. AUTHOR(s) S. A. Collins Jr.		8. CONTRACT OR GRANT NUMBER(s) F30602-72-C-0305
		10. PROGRAM ELEMENT, PROJECT, TASK AREA & WORK UNIT NUMBERS 02301E, 1279, 02, 05
9. PERFORMING ORGANIZATION NAME AND ADDRESS Ohio State Univ Electroscience Lab Department of Electrical Engineering Columbus, OH		12. REPORT DATE September 1973
		13. NUMBER OF PAGES 17 25
11. CONTROLLING OFFICE NAME AND ADDRESS Defense Advanced Research Projects Agency Washington, DC		15. SECURITY CLASS. (of this report) UNCL
		15a. DECLASSIFICATION/DOWNGRADING SCHEDULE N/A
14. MONITORING AGENCY NAME & ADDRESS (if different from Controlling Office) Rome Air Development Center Environmental Studies Section (OCSE) Griffiss AFB NY 13441		
16. DISTRIBUTION STATEMENT (of this Report) Approved for public release, distribution unlimited		
17. DISTRIBUTION STATEMENT (of the abstract entered in Block 20, if different from Report)		
18. SUPPLEMENTARY NOTES		
19. KEY WORDS (Continue on reverse side if necessary and identify by block number) atmospheric imaging image restoration propagation image processing		
20. ABSTRACT (Continue on reverse side if necessary and identify by block number) This report presents a study of problems associated with using the Fourier transform restoration procedure to restore atmospherically degraded images of high flying objects. The study is divided into two parts, an examination of the restoration procedure and an estimate of atmospheric effects. The two parts were joined by choosing a model which assumes the phase front of an atmospherically degraded light wave can be represented as a		

DD FORM 1 JAN 73 1473

EDITION OF 1 NOV 65 IS OBSOLETE

UNCLASSIFIED

SECURITY CLASSIFICATION OF THIS PAGE (When Data Entered)

UNCLASSIFIED

SECURITY CLASSIFICATION OF THIS PAGE(When Data Entered)

20. truncated polynomial series. Preliminary results indicate that a point source on the bottom of an airplane is very nearly equivalent to a collimated source at the same location as far as ability to restore the degraded image of a much higher object.

ib

UNCLASSIFIED

SECURITY CLASSIFICATION OF THIS PAGE(When Data Entered)

INVESTIGATION OF LASER PROPAGATION PHENOMENA

S. A. Collins, Jr.

Contractor: Ohio State University
Contract Number: F30602-72-C-0305
Effective Date of Contract: 1 April 1972
Contract Expiration Date: 30 September 1973
Amount of Contract: \$75,000.00
Program Code Number: 1E20

Principal Investigator: Dr. Stuart A. Collins, Jr
Phone: 614 422-5054

Project Engineer: Edward K. Damon
Phone: 614 422-5953

Contract Engineer: Raymond P. Urtz, Jr.
Phone: 315 330-3145

Approved for public release;
distribution unlimited.

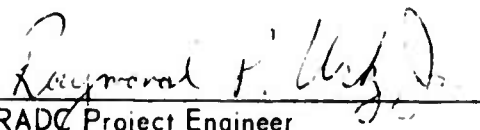
This research was supported by the
Defense Advanced Research Projects
Agency of the Department of Defense
and was monitored by Raymond P. Urtz,
Jr. RADC (OCSE), GAFB, NY 13441 under
Contract F30602-72-C-0470.

ic

NOV 72
E

PUBLICATION REVIEW

This technical report has been reviewed and is approved.



RADG Project Engineer

ABSTRACT

This report presents a study of problems associated with using the Fourier transform restoration procedure to restore atmospherically degraded images of high flying objects. The study is divided into two parts, an examination of the restoration procedure and an estimate of atmospheric effects. The two parts were joined by choosing a model which assumes the phase front of an atmospherically degraded light wave can be represented as a truncated polynomial series. Preliminary results indicate that a point source on the bottom of an airplane is very nearly equivalent to a collimated source at the same location as far as ability to restore the degraded image of a much higher object.

TABLE OF CONTENTS

	Page
I. INTRODUCTION	1
II. IMAGE PROCESSING EFFECTS	4
III. IMAGE EVALUATION CRITERIA	6
IV. IMAGE PROCESSING STUDIES RESULTS	7
V. ATMOSPHERIC EFFECTS	11
VI. SUMMARY	16

I. INTRODUCTION

This is the fourth quarterly technical report for contract No. F30602-72-C-0305. The object of the program is to provide theoretical studies of selected topics associated with light-beam propagation through a turbulent atmosphere. The present problem of interest has to do with atmospheric imaging and image restoration. It is an examination of the effectiveness of point and other types of reference sources for image restoration in the cases where the restoration reference source and object are not necessarily at the same range and position as the object. The general area is of particular interest to those interested in taking precision photographs of earth satellites with ground-based telescopes. It may also be of interest to those considering doing long distance imaging of terrestrial objects.

The work presented in this report is based on a familiar procedure for image restoration: the Fourier transform procedure (Harris, 1966). There, one images simultaneously a turbulence degraded object and a turbulence degraded point reference source. If every point in the object and the point reference source are degraded exactly the same, then the quotient of the degraded object spatial spectrum and the reference point spatial spectrum is the restored image spatial spectrum. This is the ideal case. The investigation reported herein considers the situation where the reference source is different in location and has slightly different degradation from that of the ideal situation.

The situation of interest is shown in Fig. 1. We consider two point sources, possibly at different distances from an imaging telescope. The light from the two sources travels through a turbulent atmosphere and is imaged on two image planes appropriate to their distances. One then records the instantaneous intensity patterns and uses them with the appropriate transverse size scaling in the Fourier transform restoration procedure.

The restoration procedure in this situation is expected to have limitations. The situation becomes complicated if 1) the object points and reference point are not at the same transverse location so that rays from the two partly intersect areas of different index fluctuations, and 2) the object and point reference sources are at different distances from the receiver so that refractive index fluctuations of a given size experience different magnifications by the time they have arrived at the receiver.

One way to overcome the limitation arising when the object is at infinity and the reference source is at a finite distance from the receiver is to use a collimated rather than a power reference source. This would duplicate the point source at infinite distance and should work if the degrading turbulence is between the reference source and the receiver.

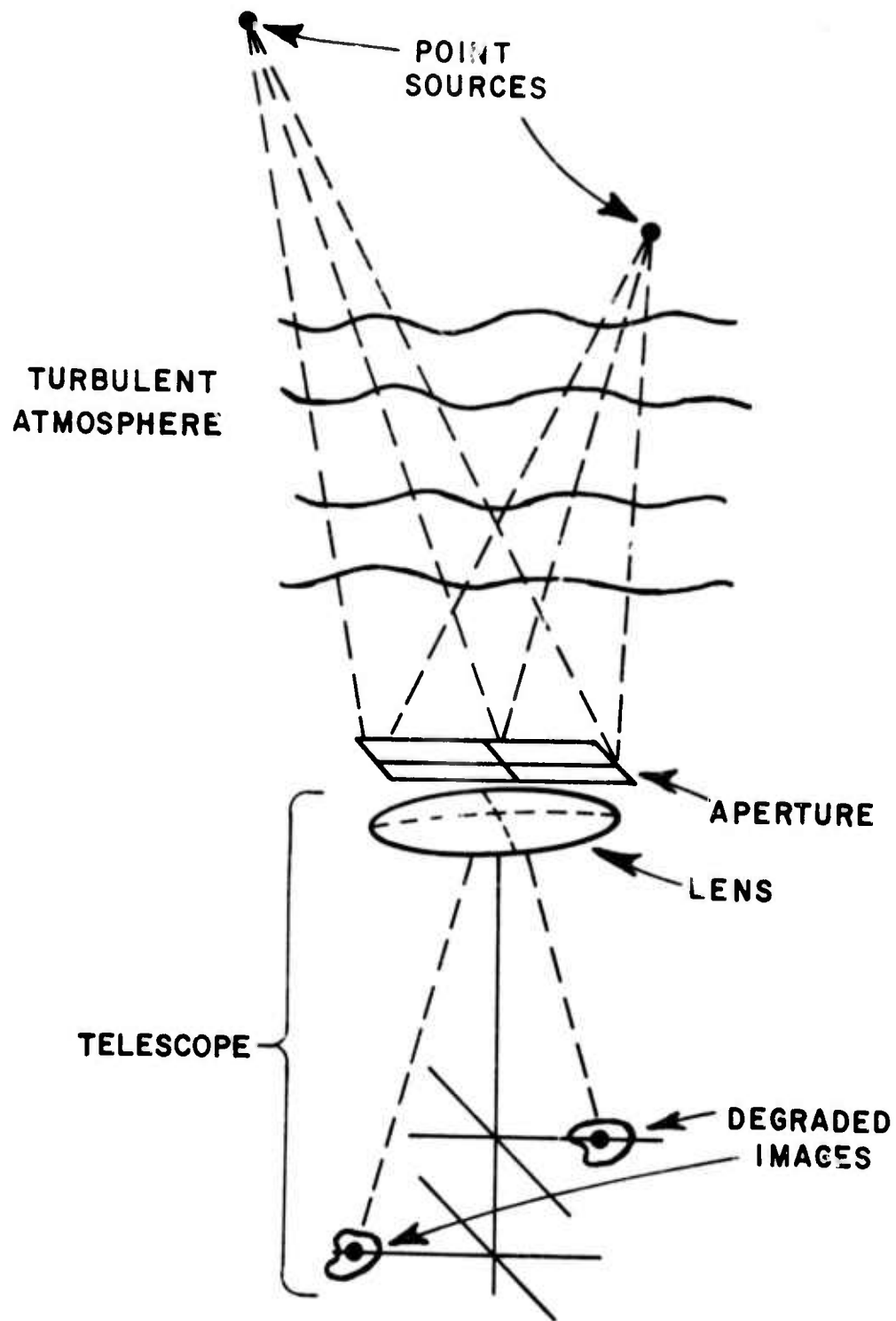


Fig. 1. Schematic illustration of physical situation.

The problem considered in these calculations is to assess the effects of displacement of the reference source and to determine the feasibility of using the plane-wave source as a possible remedy in overcoming the effects of longitudinal distance difference.

A model is chosen which allows the problem to be greatly simplified. The model is characterized by the assumption that the effect of the atmospheric turbulence on the wavefront of the light arriving at the imaging telescope aperture can be represented by deviations from the non-turbulent situation. These deviations are described mathematically in terms of a series of polynomials in transverse position, \bar{r} , which indexes the deviation at any given aperture position. Thus we represent the phase, ϕ , of the light arriving at position \bar{r} in the aperture from a given source in the form

$$(1a) \quad \phi(\bar{r}) = \phi_0(\bar{r}) + \phi_1(\bar{r})$$

where

$$(1b) \quad \phi_1(\bar{r}) = \sum_n a_n F_n(\bar{r})$$

and where ϕ_0 represents the phase in the ideal (non-turbulent) case and $\phi_1(\bar{r})$ represents the atmospherically induced fluctuations. The polynomial series similar to that used by Fried (Fried, 1967) will be given later.

The approach to the problem has two parts, both of which can be stated in terms of the quantities in Eqs. (1). In the first part, the Fourier transform restoration procedure is carried out using a particular model for the object and reference input plane field. In the model these fields are represented using one or more terms in the series in Eq. (1b), thus representing particular wavefront deviations. Indeed for the case considered, one polynomial (the same one) is used for both the object and reference beam phases. The two wavefronts differ in the size of the coefficients a_n and a_n' multiplying the polynomials; i.e., they have the same-shaped wavefront deviation but one is more bent than the other. The quality of the restoration is then investigated as a function of the difference between the coefficients. This allows a limit to be set on the size of the coefficient difference before the restoration procedure breaks down.

The coefficient difference is further related to the atmospheric parameters. Specifically, the root-mean-square coefficient difference is calculated as a function of object-to-reference source separation, range, wavelength, turbulence strength, and receiving plane aperture size, etc.

The combination of the image processing and atmospheric calculations for the coefficient difference then allows one to calculate an index of successful restoration for a given set of atmospheric parameters.

It is assumed that the signal-to-noise ratio is sufficiently large so as to allow complete recording of all pertinent images.

In a previous report (3432-4) the analysis of the restored image spectrum in the first part of the analysis was started. The work presented in this report extends the part of the effort concerned with image restoration studies. The work presented also represents the beginning of the other part of the effort, the atmospheric part.

The material presented in this report is by no means complete but summarizes work in progress. It draws on two other reports: 3432-5 which covers the restoration studies in more detail, and 3432-7 which presents the details of the atmospheric calculation. Further, neither of these reports represents a completed work, but both present detailed calculations from which preliminary results may be drawn.

In section II of this report, the Fourier transform restoration procedure is applied to images formed with wavefront image degradation determined by one or another of the wavefront polynomials. An expression for the restored image spectrum is stated under the assumption that only the first six polynomials in the series have significant effect. In section III three criteria for restored image evaluation are presented. Section IV contains examinations of restored images using the three image criteria as the difference in polynomial coefficients is increased. This leads to possible estimates of upper limits on the wavefront differences. Section V contains an analysis of the wavefront deviation determined by particular atmospheric conditions. The effects of standard ground layer turbulence are considered, as are those of a strong turbulent layer. The summary is in section VI.

II. IMAGE PROCESSING EFFECTS

In this section we examine the results of applying the Fourier transform restoration procedure to images degraded by the addition of the particular polynomial shape to the incoming ideal electric field phase. The restored images are compared using several different criteria to give information about allowable wavefront differences.

The approach follows that introduced in the previous quarterly report (3432-4). The electric fields arriving at the input aperture from both the object and reference point sources are assumed to have the form

$$(2) \quad E = E_0 \exp(j\phi(\bar{r}))$$

where $\phi(\bar{r})$ is given by Eqs. (1). The orthonormal polynomials used are, up to the second order,

$$(3a) \quad F_1 = \frac{1}{a}$$

$$(3b) \quad F_2 = \frac{\sqrt{3}}{a} \frac{x}{a/2}$$

$$(3c) \quad F_3 = \frac{\sqrt{3}}{a} \frac{y}{a/2}$$

$$(3d) \quad F_4 = \frac{1}{a} \frac{3}{2} \sqrt{\frac{5}{2}} (x^2 + y^2 - (a^2/6))/(a/2)^2$$

$$(3e) \quad F_5 = \frac{1}{a} \frac{3}{2} \sqrt{\frac{5}{2}} (x^2 - y^2)/(a/2)^2$$

$$(3f) \quad F_6 = (3/a)(xy)/(a/2)^2$$

These polynomials are chosen so as to be orthonormal over a square aperture of side "a". It is assumed that the major effect of the atmosphere is represented by the first six polynomials, an assumption born out (at least in the mean square sense) by our calculations and by Fried.

The first step in using the polynomial procedure is to calculate an expression for the restored image spectrum assuming the input light field described in Eq. (2). This involves first finding the field correlation functions of the object and reference fields. These represent the spatial spectra of the associated object and reference image intensities. The quotient of these two spectra is the spatial spectrum of the restored image. The expression for the restored image spectrum is then (3432-4),

$$(4a) \quad W_0(\bar{\kappa}) = \frac{W(\bar{\kappa})}{W'(\bar{\kappa})} \cdot e^{j(\phi_0 - \phi_0')} \times \frac{(B'_{xx}\kappa_x + B'_{xy}\kappa_y)(B'_{yy}\kappa_y + B'_{xy}\kappa_x)}{(B_{xx}\kappa_x + B_{xy}\kappa_y)(B_{yy}\kappa_y + B_{xy}\kappa_x)}$$

$$\times \frac{\sin|((ka/d) - |\kappa_x|)(B_{xx}\kappa_x + B_{xy}\kappa_y)| \sin|((ka/d) - |\kappa_y|)(B_{yy}\kappa_y + B_{xy}\kappa_x)|}{\sin|((ka/d) - |\kappa_x|)(B'_{xx}\kappa_x + B'_{xy}\kappa_y)| \sin|((ka/d) - |\kappa_y|)(B'_{yy}\kappa_y + B'_{xy}\kappa_x)|}$$

$$- \frac{ka}{d} < \kappa_x < + \frac{ka}{d}$$

$$- \frac{ka}{d} < \kappa_y < + \frac{ka}{d}$$

where the quantities B_{xx} , B_{xy} , B_{yy} and ϕ_0 are related to the wavefront deformation parameters, a_2 through a_6 by^o

$$(4b) \quad \phi_0 = 2\sqrt{3}(d/a^2k)(a_2\kappa_x + a_3\kappa_y)$$

$$(4c) \quad B_{xx} = 6\sqrt{5/2} (a_4 + a_5) (d/2k)^2/(a/2)^3$$

$$(4d) \quad B_{xy} = B_{yx} = 6a_6(d/2k)^2/(a/2)^3$$

$$(4e) \quad B_{yy} = 6\sqrt{5/2} (a_4 - a_5) (d/2k)^2/(a/2)^3 .$$

The primes indicate the coefficients for the reference beam, the unprimed variables are for the object beam. Of the other quantities, $k = 2\pi/\lambda$, where λ is the light wavelength, "a" is the size of the square telescope receiving aperture, "d" is the telescope image distance, and κ_x and κ_y are spatial frequency components.

It is to be noted that if the object and reference wavefronts are identical; i.e. $a_n = a_n'$, then all the primed and unprimed quantities are equal respectively, and $W_0(\bar{\kappa})$ is equal to unity.

It is also noted that the linear wavefront tilt terms a_2 and a_3 produce only translation of the restored image since they only appear in the spatial spectrum as the factor $e^{j(\phi_0 - \phi_0')}$. With an extended object these would move points around, but not degrade resolution. For this reason effort is concentrated on estimating the effect of the quadratic wavefront distortion terms indexed by the B_{ij} and B'_{ij} .

The expression in Eq. (4) is evaluated using selected values for the parameters. It is digitally Fourier transformed and the resulting two-dimensional images are examined using several different criteria.

III. IMAGE EVALUATION CRITERIA

Three different criteria were used to evaluate the restored images. They are the restored image Strehl ratio, the normalized integral scale width, and the mean square difference from the ideal restored image. These criteria give respectively measures of the restored image contrast, the restored image resolution, and the intensity difference from the ideal case. The mean square error is included because it is conceivable that the Strehl ratio which is proportional to the integral over spatial frequency space of the restored image spectrum might have a reasonable value even though the restored image spectrum was fluctuating wildly but having nearly equal positive and negative parts. This would give a reasonable Strehl ratio but a poor restored image. Similar behavior could occur for the integral scale.

Numerical values were chosen to indicate whether an image was properly restored according to these criteria. Specifically, for the Strehl ratio and the normalized integral scale width, they were "three db" points. Thus if the Strehl ratio and normalized integral scale of the restored image were between 0.5 and 2.0, the image was termed acceptably restored. Similarly, a mean square deviation of 0.1 or less was termed acceptable.

IV. IMAGE PROCESSING STUDIES RESULTS

The details of the calculation of the restored images and the evaluation of the three measures of the image quality are given in another report (3432-5). In order to understand the detailed behavior of these three quantities, it was necessary to examine in detail the locations of the poles and zeros of the restored image spectrum. Indeed, the one most significant factor in determining the behavior of these quantities was the change of these poles and zeros with the size of the a_n , the wavefront polynomial coefficients. These factors are covered in detail in report 3432-5.

The results of the restored image evaluation are presented in a particular form. Implicit is the assumption that both the object and reference fields are assumed to be perturbed by the same shape functions. They differ in the amount of one function. The wavefront deformation is represented by the coefficients a_n , and a_n' for the object and reference values, respectively. A particular value is chosen for one of the coefficients, say a_m and a slightly different value is chosen for a_m' , the difference being designated by Δa_m where $\Delta a_m = a_m' - a_m$. The image evaluation criteria are then plotted as a function of Δa_m . Thus, in the case where $\Delta a_m = 0$, there may be considerable degradation, i.e., large values of the a_n , but still perfect restoration.

One case is shown here, a case where all but a_4 and a_4' are zero, these coefficients representing focusing errors. The case chosen has an object wavefront deviation of three-quarters of a wavelength at the aperture edge on axis, a value sufficiently large so as to give observable degradation.

The restored image Strehl ratio, integral scale and mean square errors are shown in Figs. 2a, 2b and 2c, respectively, plotted as a function of wavefront difference at the aperture edge on axis. There are several items of interest in these figures. First consider the Strehl ratio as shown in Fig. 2a. We see that when there is no wavefront difference, $\Delta a_4 = 0$, the Strehl ratio, S_r , equals one as it should. For values of Δa_4 between -0.003 and +0.005 there is acceptable restoration. For values of S_r outside that region there are alternating regions of unacceptable restoration, indicated by the cross-hatched areas, and acceptable restoration. It is worthwhile pointing out the fact that the image quality does not slowly deteriorate and then stay bad, but has alternating bad and good regions. Similar behavior occurs for the integral scale and mean square error.

Reproduced from
best available copy.

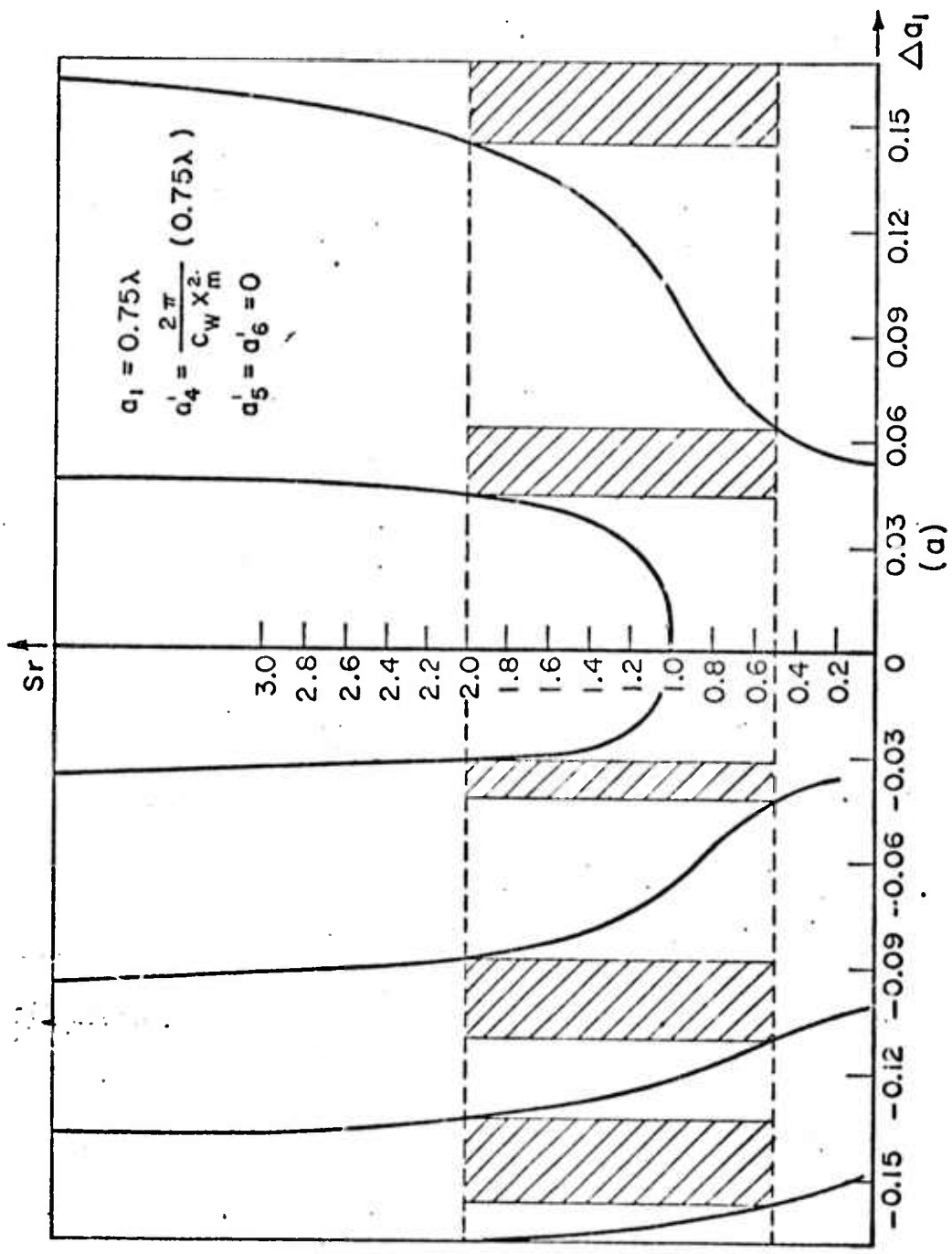


Fig. 2a. Graph of restored image Strehl ratio versus wavefront difference for object-wavefront deviation of three-quarters of a wavelength.

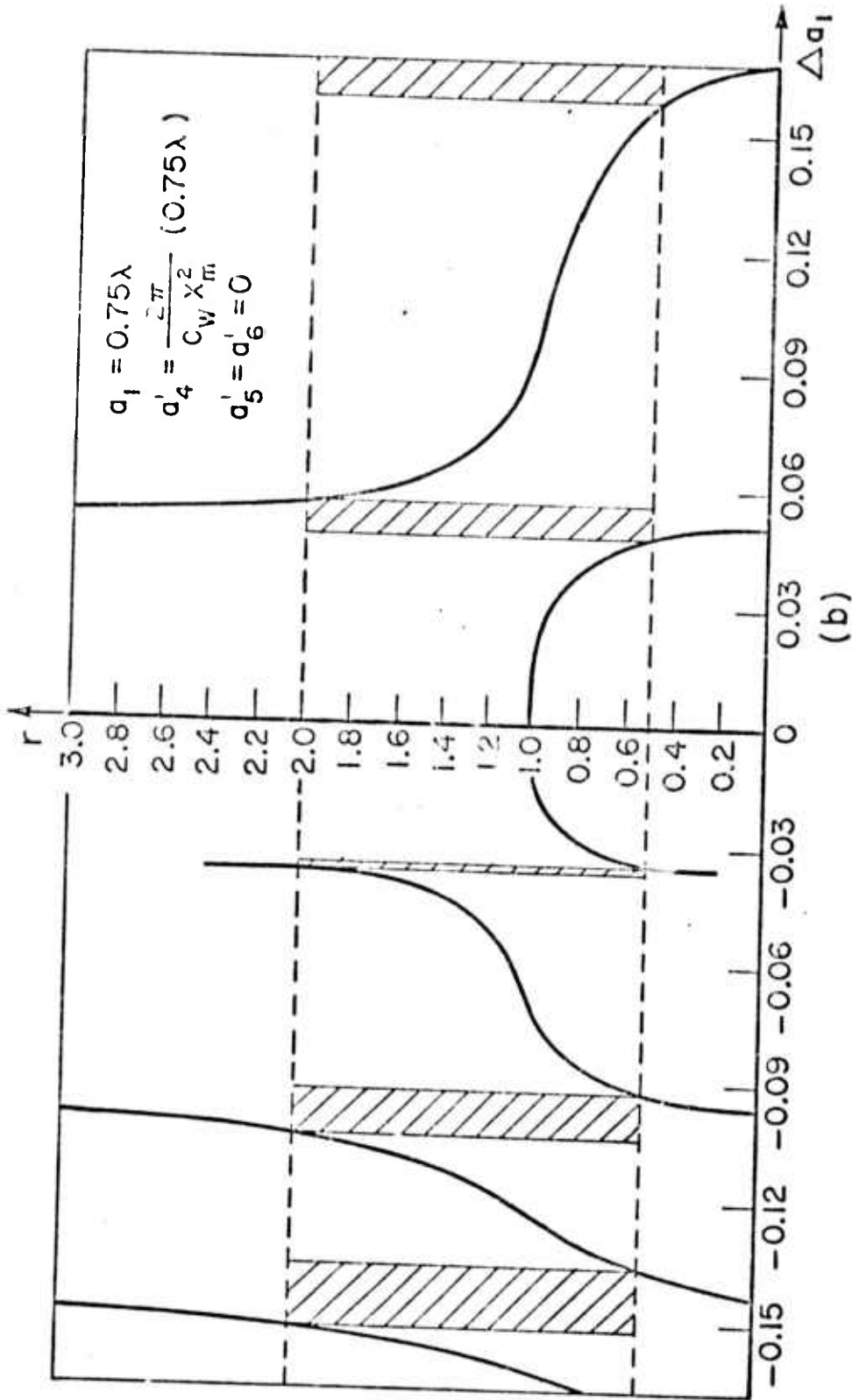


Fig. 2b. Graph of normalized restored image integral scale width versus wavefront difference for object wavefront deviation of three quarters of a wavelength.

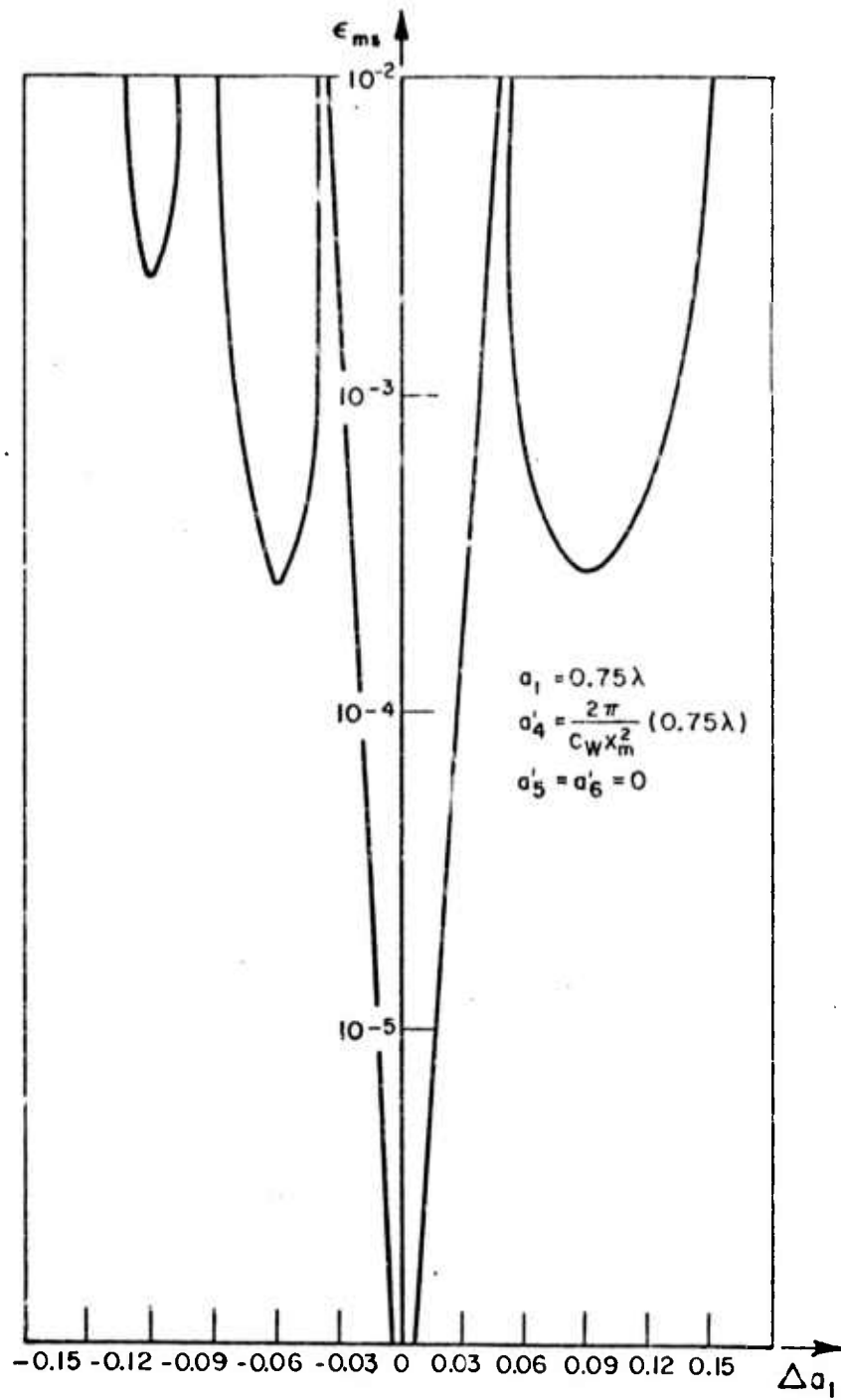


Fig. 2c. Graph of mean squared error versus wavelength difference for object wavefront deviation of three quarters of a wavelength.

Also of interest is that the restored image spectrum and the restoration process depend on the number of wavelengths deviation of the image wave itself. That variation also is not monotonic in nature. Further, graphs given in report 3432-5 show that for 0.5 wavelengths deviation at the aperture edge on axis, there is difficulty in restoring the image because of the number of poles and the way they move with respect to the sampling points. The case is worse than for the one and one-half wavelengths case shown here. On the other hand, the case where there is a half-wave variation for the image plane wavefront on axis is relatively easy to restore.

It should be noted that the data presented in Figs. 2 was obtained by a dogmatic application of the Fourier transform procedure. No attempt was made to smooth or clip the restored image spectrum. There is a significant question as to whether the discrete representation used has a sufficiently fine point spacing to faithfully represent the function without some smoothing, and meaningfully with smoothing.

To summarize, the Fourier transform restoration procedure has been applied to simple point object and reference images with simple variation of the wavefront from ideal. Using the Fourier transform procedure with no restored image spectrum smoothing, an examination was conducted to see how much difference could be allowed between the object and reference wavefronts before restoration became impossible. Typical numbers are .003 wavelengths difference at the edge to assure restoration, and larger than 0.1 wavelengths if one accepts alternating regions of restorable and non-restorable images.

V. ATMOSPHERIC EFFECTS

In this section a study is made of the size of the maximum wavefront deviation of the spherical and other components due to atmospheric refractive index effects. The input information comprises physical parameters such as ranges, separation of the point sources, and variation of the refractive index fluctuations. The questions asked relate to the root-mean-square values of the atmospherically induced variation of the coefficients in the wavefront polynomial series for three source configurations and for ground level turbulence and high altitude turbulent layers. The calculation uses the (reasonable) assumption that phase effects are predominant, and neglects amplitude effects. Results will be summarized here, and the details presented in a different report (3432-7).

The physical situation considered in the analysis is shown in Fig. 3. There we see two point sources located at points \bar{r} and $\bar{r}+\bar{\rho}$. The phase variations from ideal of the light arriving at the input aperture from the two sources are, respectively, $\phi_1(\bar{r}_1, \bar{r})$ and $\phi_1(\bar{r}_1, \bar{r}+\bar{\rho})$ given by

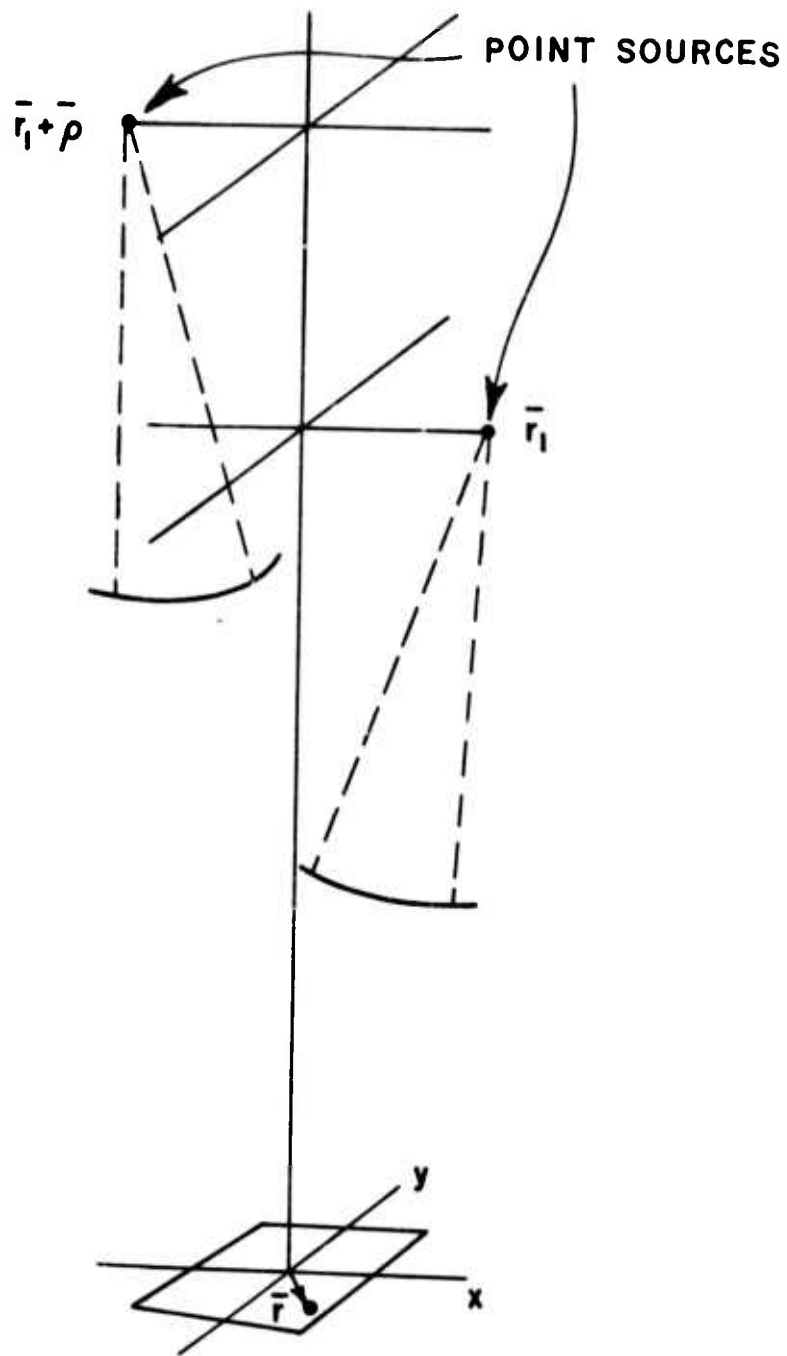


Fig. 3. Schematic illustration of physical situation showing variable definitions.

$$(6a) \quad \phi_1(\bar{r}, \bar{r}_1) = \sum a_n(\bar{r}_1) F_n(\bar{r})$$

and

$$(6b) \quad \phi_1(\bar{r}, \bar{r}_1 + \rho) = \sum a_n'(\bar{r}_1 + \rho) F_n(\bar{r})$$

The light from the two sources may travel through regions of different atmospheric index fluctuations, and therefore have different series represented by the $a_n(\bar{r}_1)$ and $a_n'(\bar{r}_1 + \rho)$.

The quantity of interest is the root-mean-square coefficient difference,

$$(7) \quad \sqrt{D_a(\rho)} = \sqrt{\langle |a_n'(\bar{r}_1 + \rho) - a_n(\bar{r}_1)|^2 \rangle}$$

where the brackets represent ensemble averaging.

The input formulae used for the calculation of $\sqrt{D_a(\rho)}$ are the definition of the a_n based on the fact that the polynomials $F_n(\bar{r})$ are orthonormal over a square aperture of side "a"

$$(8) \quad a_n = \iint F_n(\bar{r}) \phi_1(\bar{r}) W(\bar{r}) d\bar{r}$$

($W(\bar{r})$ is the aperture function equal to 1 inside the aperture and 0 outside it), the expression for the phase

$$(9) \quad \phi_1 = k \int_0^L n(\bar{r}') dz$$

and the expression for the index structure function,

$$(10) \quad D_n(\bar{r}' - \bar{r}'') = C_n^2 |\bar{r}' - \bar{r}''|^{2\beta}$$

Combining Eqs. (7), (8), (9), and (10) gives the basic expression for $\sqrt{D_a(\rho)}$.

$$(11a) \quad \sqrt{D_a(\rho)} = \left\{ \iint d\bar{r} d\bar{r}' F_n(\bar{r}) F_n(\bar{r}') W(\bar{r}) W(\bar{r}') D_\phi(\bar{r} - \bar{r}', \rho) \right\}^{\frac{1}{2}}$$

where

$$(11b) \quad D_{\phi}(\bar{r}-\bar{r}', \rho) = \frac{k^2}{2} \int_0^L \int_0^L dz_1 dz_2 \left[D_n(\rho_1-\rho_2', z_1-z_2) \right. \\ \left. + D_n(\rho_2-\rho_1', z_1-z_2) - D_n(\rho_1-\rho_2, z_1-z_2) - D_n(\rho_2-\rho_2', z_1-z_2) \right]$$

The integrals in Eq. (11) are simplified and then evaluated using a digital computer. The details are presented in report 3432-7; only typical results will be presented here. Such results are shown in Fig. 4 where we see $\sqrt{D_{a_4}(\rho)}$ graphed as a function of ρ for point objects at 20 km and 150 miles and point reference at 20 km, and for two turbulent conditions. The two bottom curves show the effects of surface level turbulence ($C_n^2(z) = (z/z_0)^{-4/3}$) for the two different objects and the two top curves show the effects of a high altitude turbulence layer at 17 km. These curves apply specifically for coefficient a_4 ; however, similar curves are shown for a_5 and a_6 in report 3432-7.

The strength of the turbulent layer was chosen so as to provide the same value for a plane wave wave-structure function at the ground for a point source at infinite range and turbulent layer, as due to ground level turbulence, and point source at infinity. The calculations were made for $\lambda = 0.5 \mu$ and $C_n^2 = 2.1 \times 10^{-16}$ at one meter height.

The curves exhibit some expected behavior. For the cases where point object and reference are both at 20 km height, $\sqrt{D_{a_4}(\rho)}$ goes to zero as ρ becomes small. This is expected since light from both (point) sources ends up traversing regions of the same refractive index fluctuations. For the case where one source is at a different height than the other, there is a residual value for $\sqrt{D_{a_4}(0)}$ even when $\rho = 0$. This is because a given index fluctuation magnifies light differently from sources at different distances, and there is complete cancellation only for very low level turbulent fluctuations. It is also noted that the effect of the high-level turbulent layer is significantly greater than that due to the ground level turbulence. That is, a small separation of rays from the two sources produces a much greater effect in interacting with high level index fluctuations than with ground level fluctuations, due to the wavefront magnification of spherical waves.

The curves can be useful in deciding whether restoration is possible in a given situation. For example, if a value of 0.01 wavelengths difference can be tolerated for the wavefronts then a very close spacing between reference and image must be obtained or there must be weaker turbulence. If a value of 0.10 is acceptable, then, with the value of C_n^2 chosen, a source separation of one aperture size is allowed.

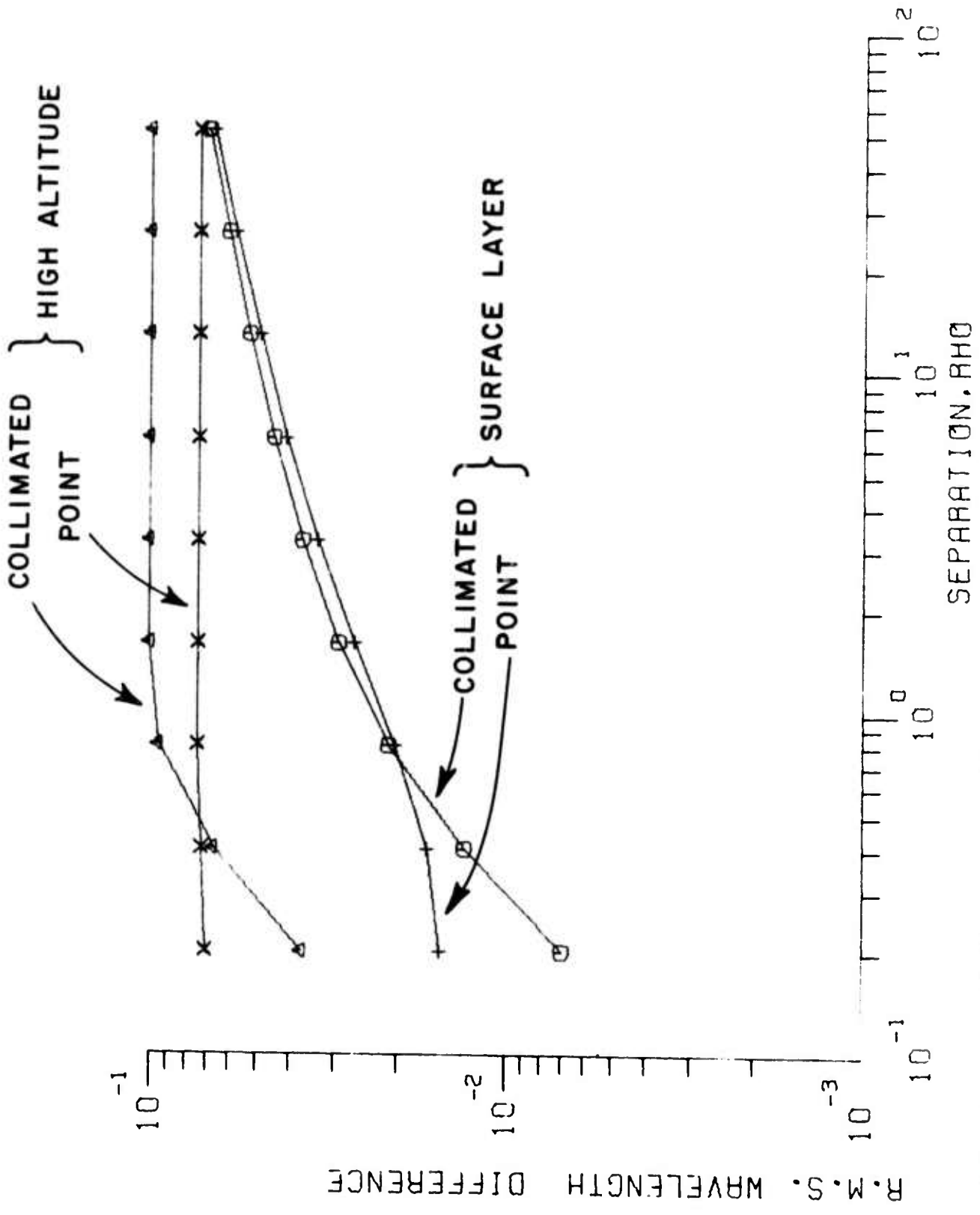


Fig. 4. Graph of RMS wavefront difference versus object-reference source distance.

One other point is indicated. That concerns the relative ease of restoration for objects at the same height as the reference, as for an object much higher than the reference. Fig. 3 indicates that for object and reference separated by more than one aperture size, the ease of restoration is almost the same, the values of $\sqrt{D_{au}(\rho)}$ lying within a factor of two of each other for $\rho/a \geq 1$.

To summarize this section, the root-mean-square coefficient difference induced by turbulent index fluctuations has been calculated. Results indicate that high altitude turbulence effects are somewhat stronger than those due to ground layer turbulence. Further, the ability to restore is about the same for an object at the reference source height as it is for an object much higher than the reference source for very reasonable separations between object and reference. RMS coefficient values between 10^{-3} and 10^{-1} wavelengths are to be expected.

VI. SUMMARY

Summarizing the results of the report, the problem of using the Fourier transform restoration procedure to restore atmospherically degraded images was divided into two parts, a study of the restoration procedure, and a study of atmospheric effects. The two parts were joined by choosing a model which assumes the phase front of an atmospherically degraded light wave can be represented as a truncated polynomial series. The effects of a wavefront shape represented by one term of the series was examined, in this case the shape representing atmospherically defocused images. Preliminary results indicate that the effects of wavefront differences between object and reference beams are not simply described, being an alternating function of wavefront difference and not a monotonic function. Wavefront differences of less than .003 wavelengths assure restoration effectiveness, while much larger wavefront differences may allow restoration.

As far as atmospheric effects are concerned, root-mean-square wavefront differences of .001 to .01 wavelengths are reasonable for medium strength ground-level turbulence. High altitude turbulence layers and strong ground level turbulence may make restoration impossible. A point reference source is nearly as effective in restoring the image of an object at the height of the reference source as it is in restoring an object at a much greater height. High altitude turbulence is somewhat more effective in preventing the restoration process than is ground-level turbulence.

Further work needs to be done in examining the polynomial series representation employed, in using smoothing in the restored imaging spectrum, and in extending quoted results to other cases.

REFERENCES

- Fried, 1965, Davis L., "Statistics of a Geometric Representation of Wavefront Distortion," J. Opt. Soc. Am. 55, 1427.
- Harris, 1966, James L., Sr., "Image Evaluation and Restoration," J. Opt. Soc. Am. 56, 569.
- Collins, 1973, Stuart A., "Investigation of Laser Propagation Phenomena," Report 3432-4, The Ohio State University ElectroScience Laboratory, Department of Electrical Engineering; prepared under Contract F30602-72-C-0305 for Rome Air Development Center. (RADC-TR-73-115) (AD 760 548)
- Davidson, 1973, R. S. II, "A Study of the Fourier Transform Method of Image Restoration," Report 3432-5, The Ohio State University ElectroScience Laboratory, Department of Electrical Engineering; prepared under Contract F30602-72-C-0305 for Rome Air Development Center.
- Collins, 1973, Stuart A., ElectroScience Laboratory Report in process.